




ORIGINAL ARTICLE

Greater extent of blood-tumor TCR repertoire overlap is associated with favorable clinical responses to PD-1 blockade

Hiroyasu Aoki^{1,2}  | Satoshi Ueha¹  | Yoshiaki Nakamura^{3,4} | Shigeyuki Shichino¹ | Hiromichi Nakajima^{4,5} | Manami Shimomura⁵ | Akihiro Sato⁶ | Tetsuya Nakatsura⁵  | Takayuki Yoshino⁴ | Kouji Matsushima¹

¹Division of Molecular Regulation of Inflammatory and Immune Diseases, Research Institute for Biomedical Sciences, Tokyo University of Science, Noda City, Japan

²Department of Hygiene, Graduate School of Medicine, The University of Tokyo, Tokyo, Japan

³Translational Research Support Section, National Cancer Center Hospital East, Kashiwa City, Japan

⁴Department of Gastroenterology and Gastrointestinal Oncology, National Cancer Center Hospital East, Kashiwa City, Japan

⁵Division of Cancer Immunotherapy, Exploratory Oncology Research & Clinical Trial Center (EPOC), National Cancer Center, Kashiwa, Japan

⁶Clinical Research Support Office, National Cancer Center Hospital East, Kashiwa City, Japan

Correspondence

Satoshi Ueha, Division of Molecular Regulation of Inflammatory and Immune Diseases, Research Institute for Biomedical Sciences, Tokyo University of Science, 2669 Yamazaki, Noda City, Chiba 278-0022, Japan.
Email: ueha@rs.tus.ac.jp

Funding information

This work was supported by Grants-in-Aid for Scientific Research (B) 20281832, Grant-in-Aid for Scientific Research on Innovative Areas 17929397, and ONO Pharmaceutical Co., Ltd. We would like to thank M. Tsunoda for technical assistance. H. Aoki was supported by the Tamamitsu Kishimoto Fellowship Program. We would like to thank Editage (www.editage.com) for English language editing.

Abstract

With the widespread use of programmed death receptor-1 (PD-1) blockade therapy, sensitive and specific predictive biomarkers that guide patient selection are urgently needed. T-cell receptor (TCR) repertoire, which reflects antitumor T-cell responses based on antigen specificity, is expected as a novel biomarker for PD-1 blockade therapy. In the present study, the TCR repertoire of eight patients with gastrointestinal cancer treated with anti-PD-1 antibody (nivolumab) was analyzed. To analyze the tumor-associated T-cell clones in the blood and their mobilization into the tumor, we focused on T-cell clones that presented in both blood and tumor (blood-tumor overlapping clones). Responders to PD-1 blockade tended to exhibit a higher number of overlapping clones in the tumor and a higher total frequency in the blood. Moreover, a higher total frequency of overlapping clones in blood CD8⁺ T cells before treatment was associated with a favorable clinical response. Collectively, these results suggest the possibility of blood-tumor TCR repertoire overlap to predict clinical response to PD-1 blockade and guide patient selection before the treatment.

KEYWORDS

blood-tumor overlapping clone, immune checkpoint inhibitor, PD-1 blockade, TCR repertoire

Abbreviations: CDR3, complementarity-determining region 3; dLN, tumor-draining lymph node; ICI, immune checkpoint inhibitor; J segment, joining segment; PC1, principal component 1; PD, progressive disease; PD-1, programmed death receptor-1; PD-L1, programmed death-ligand 1; PR, partial response; SD, stable disease; TCR, T-cell receptor; TIL, tumor-infiltrating lymphocyte; TMB, tumor mutational burden; V segment, variable segment.

Clinical trial registration information: Patients enrolled in a multicenter phase II study of nivolumab monotherapy in advanced gastrointestinal cancer patients with high tumor mutation burden (TMB-H) (UMIN000033182) were analyzed in this study. Ethics approval and consent to participate: The study was conducted in accordance with the Declaration of Helsinki and Good Clinical Practice Guidelines, following approval by the ethics board in each institution. All patients provided written informed consent for participation in the study.

Aoki and Ueha contributed equally.

This is an open access article under the terms of the Creative Commons Attribution-NonCommercial License, which permits use, distribution and reproduction in any medium, provided the original work is properly cited and is not used for commercial purposes.

© 2021 The Authors. *Cancer Science* published by John Wiley & Sons Australia, Ltd on behalf of Japanese Cancer Association.

1 | INTRODUCTION

With the widespread use of immune checkpoint inhibitors (ICIs) for cancer therapy, including anti-programmed death receptor-1 (PD-1)/programmed death-ligand 1 (PD-L1) monoclonal antibodies, a biomarker that guides patient selection is urgently needed. The density of tumor-infiltrating lymphocytes (TILs)¹ or expression level of PD-L1 in the tumor,² which represents the existence of an immune response, have been reported as predictive factors for the efficacy of PD-1 blockade. Tumor mutational burden (TMB), which may reflect the immunogenic potential of the tumor,³ is also a novel candidate. However, the sensitivity and specificity of these factors are low.⁴ Given the mode of action, the strength of antitumor T-cell responses, determined by the amount and variety of tumor-specific T cells, is an essential factor for responsiveness to PD-1 blockade. Therefore, indices reflecting tumor-specific T-cell responses would be ideal biomarkers to predict and diagnose patient response to PD-1 blockade.

Tumor-specific T cells recognize cancer antigens via the T-cell receptor (TCR), which determines the specificity of T cells, and then undergo clonal expansion. Thus, the TCR repertoire, the collection of TCRs in tumor-bearing hosts, reflects antitumor T-cell responses based on antigen specificity and is a potential biomarker for PD-1 blockade.⁵ Several clinical studies focused on the repertoire of tumor-infiltrating T cells. These demonstrated that the presence of more expanded T-cell clones in the tumor before treatment^{1,6,7} and the increase in the clonal expansion after treatment¹ are correlated with clinical response to PD-1 blockade. Another study analyzed the blood T-cell repertoire and established that the increase in the expanded clones of blood CD8⁺ T cells is also associated with response to ICIs.⁸ However, several studies reported conflicting results, and there is no consensus on how the characteristics of TCR repertoire are associated with clinical responses to ICIs.

Besides the reinvigoration of dysfunctional T cells residing in the tumor microenvironment, the importance of the replacement of tumor-reactive T-cell repertoire and mobilizing novel tumor-associated clones has recently been pointed out for PD-1 blockade therapy.^{9,10} In the series of steps generating antitumor immunity ("cancer-immunity cycle"), tumor-reactive T cells are primed in the tumor-draining lymph node (dLN) and trafficked to the tumor via blood circulation.¹¹ Based on this notion, overlapping TCR repertoire between the blood and tumor ("blood-tumor overlap") is thought to include clones being mobilized into the tumor, contributing to tumor T-cell repertoire replacement. We have demonstrated that the mobilization of tumor-reactive CD8⁺ T-cell clones into the cancer-immunity cycle by transient CD4⁺ cell depletion appears as an increase in the TCR repertoire that overlaps with the tumor, dLN, and the blood.^{12,13} In the present study, we performed a TCR repertoire analysis on eight patients treated with anti-PD-1 antibody (nivolumab), focusing on the blood-tumor overlapping clones. This study explored the possibility of TCR repertoire analysis to predict the responsiveness to PD-1 blockade therapy.

2 | MATERIALS AND METHODS

2.1 | Study design

The blood T cells and tumor biopsies were collected from patients enrolled in a multicenter phase II study of nivolumab monotherapy in advanced gastrointestinal cancer patients with high tumor mutation burden (TMB-H; UMIN000033182). Patients with advanced gastrointestinal cancers with high TMB confirmed by Guardant360 (Guardant Health, Inc.), a 74-gene sequencing circulating tumor DNA assay, received intravenous nivolumab monotherapy of 360 mg every 3 weeks. Computed tomography was performed at baseline and every 6 weeks thereafter until disease progression or the beginning of subsequent treatment. Tumor response was evaluated as the maximum change of sum of diameter of measurable lesions per the Response Evaluation Criteria in Solid Tumors v1.1.

2.2 | T-cell isolation from PBMCs

Ten milliliters of patient's blood was taken at four time points (P1; day 0, P2; day 21-27, P3; day 39-55, P4; disease progression). PBMCs were prepared by density gradient centrifugation by Ficoll®-Paque Plus (GE Healthcare Japan). The PBMCs were separated into two samples, and then CD8⁺ T cells and CD4⁺ T cells were enriched using CD8 MicroBeads or CD4 MicroBeads for humans (Miltenyi Biotec Inc). The purity was checked by FACSCanto II (BD Biosciences) by staining with CD8a-APC (clone RPA-T8, Tonbo Biosciences), CD3-FITC (clone UCHT1, Tonbo Biosciences), CD4-PE (clone SK3, BioLegend), and Ghost Dye Red 780 (Tonbo Biosciences). The purity of enriched cells was routinely more than 95%.

2.3 | Extraction of RNA from biopsies

Tumor biopsy was conducted before (day 0) and after the treatment (day 39-55). Presence or absence of tumor tissue in biopsies was determined pathologically. Tumor biopsies were homogenized in TRIzol (Ambion). RNA was extracted from each sample using the RNeasy mini kit (Qiagen, # 74106), and amounts and purity were measured with the Agilent 2200 TapeStation (Agilent Technologies). Five micrograms of total RNA was diluted with 1 mL of cell lysis buffer and used for TCR sequencing.

2.4 | TCR library construction and sequencing

TCR sequencing libraries for next-generation sequencing were prepared according to a previous report (GSE 115425) with some modifications.¹² PolyA RNAs were isolated according to another previous report with some modifications (GSE110711).¹⁴ To amplify the TCR cDNA containing complementarity-determining region 3 (CDR3), nested PCR of the TCR locus was performed as follows. Beads with containing cDNA

were resuspended with the first-PCR mixture composed of 0.8 μL of 10 $\mu\text{mol/L}$ primer mix (trP1, Trac_ex, and Trbc_ex), 4.2 μL of DW (distilled water), and 5 μL of KAPA Hifi HotStart ReadyMix (KAPA Biosystems, #KK2602). The thermal cycling conditions were programmed as follows: denaturation at 95°C for 3 minutes, five cycles of denaturation for 20 seconds at 98°C, annealing for 15 seconds at 65°C, and extension for 30 seconds at 72°C, followed by a final extension at 72°C for 2 minutes. Next, 10 μL of the first-PCR products were used for purification with an Agencourt AMPure XP kit (Beckman Coulter, #A63881) at a 0.7:1 ratio of beads to sample and eluted with 15 μL of DW. The second-PCR mixture consisted of 1.75 μL of 10 $\mu\text{mol/L}$ primer mix (5' WTA, Trac_in-Bio, and Trbc_in-Bio), 10.75 μL of the template, and 12.5 μL of KAPA Hifi HotStart ReadyMix. The thermal cycling conditions were the same as the first PCR except for the cycle number (21 cycles). Next, 25 μL of the second-PCR products were purified using Agencourt AMPure XP kit (Beckman Coulter) at a 0.7:1 ratio of beads to sample and eluted in 18 μL of DW. Fragmentation and adaptor ligation were performed using 10–20 ng of the second-PCR product as a template with NEBNext FS DNA Library Prep Kit (New England Biolabs, #E7805) with some modifications. NEBNext Adaptor for Illumina in the “adaptor ligation” step was substituted by 5 $\mu\text{mol/L}$ Adaptor P1, and the reaction volume was one fourth of the recommended in all steps. Adaptor-ligated DNA was purified using Agencourt AMPure XP kit (Beckman Coulter) at a 0.8:1 ratio of beads to sample and eluted in 20 μL of DW. The third PCR was carried out using barcoded primers to enrich the TCR β cDNA flanked with sequencing adapters. The third-PCR mixture consisted of 1 μL of 10 $\mu\text{mol/L}$ trP1 primer, 1 μL of 10 $\mu\text{mol/L}$ IonA-BC-Trbc primer, 3 μL of template, and 5 μL of NEBNext Ultra II Q5 Master Mix (accessory of NEBNext FS DNA Library Prep Kit). The thermal cycling conditions were programmed as follows: denaturation at 98°C for 30 seconds, 10 cycles of denaturation for 10 seconds at 98°C, and annealing and extension for 1 minute 15 seconds at 65°C, followed by a final extension at 65°C for 5 minutes. The PCR product was purified and subjected to size selection using Agencourt AMPure XP kit (Beckman Coulter) at a 1.0:1 ratio of beads to sample and eluted with 20 μL of Tris-HCl (pH 8.0). Amplified TCR β libraries were quantified using a KAPA SYBR Fast qPCR Kit (KAPA Biosystems, #KK4621), and size distribution was analyzed by agarose electrophoresis and SYBR Gold staining (Thermo Fisher Scientific, #S11494). Primers used for library preparations are summarized in Table S1.

Final TCR β libraries, whose lengths were 200–300 base pairs, were pooled and sequenced using an Ion 540 Kit Chef, an Ion 540 Chip kit, and an Ion GeneStudio S5 Sequencer (Thermo Fisher Scientific, # A27759, #A27766, # A38194) according to the manufacturer's instructions, except the input library concentration (65 pmol/L) and flow number (500). The raw data have been deposited at the NCBI GEO; accession GSE154539.

2.5 | Data processing of TCR sequencing

Adapter trimming and quality filtering of sequencing data were performed by using Cutadapt¹⁵ and PRINSEQ-0.20.4.¹⁶

Sequencing data were processed by MiXCR-3.0.5.¹⁷ In MiXCR, filtered reads were aligned to reference human TCR V/D/J sequences with the following parameters: `-vParameters.geneFeatureToAlign = VTranscript -vjAlignmentOrder = JThenV`; then, identical sequences were assembled and grouped in clones with PCR and sequencing error correlation with the following parameters: `-badQualityThreshold=10, -separateByV = true, --only-productive = true, -region-of-interest = CDR3`. The variable (V) and joining (J) segments of TCRs were represented in IMGT gene nomenclature.

The list of final clones was analyzed by VDJtools-1.2.1.¹⁸ Then, the sequencing reads of samples were normalized by the “DownSample” command of VDJtools as the following: for samples from PBMC, equal to the cell count in each sample. for tumor biopsy samples, 50 000 reads. T-cell clones were determined as TCR reads with the same TCR V segment, J segment, and CDR3 nucleotide sequence. If multiple biopsies were obtained at the same time point in a patient, TCRseq and subsequent data processing were performed separately; then, clonotype tables were pooled by the “PoolSamples” command of VDJtools. The processed data have been deposited at the NCBI GEO; accession GSE154539.

2.6 | Calculation of clonality index of TCR repertoire

The 1-Pielou index was used to evaluate the clonality of TCR repertoire, which was calculated using the formula $1 - \sum_{i=1}^n p_i \log_e(p_i) / \log_e(n)$, where p_i is the frequency of clone i for a sample with n unique clones.

2.7 | Identification of expanded and contracted clones

Significantly expanded/contracted clones were defined described in Dewitt et al,¹⁹ using Fisher's exact test on an estimated cell count of T-cell clones, including clones detected only at one time point. The estimated cell count was obtained by rounding off 100 000 times the frequency of each clone, and q values corresponding the P -values of Fisher's exact test were calculated using the `qvalue` package in Microsoft R open 3.6.0. We adopted $q < 0.01$ for threshold of expanded/contracted clones.

2.8 | Transcriptomic and quantitative real-time PCR analyses

PolyA RNAs were isolated according to a previous report with some modifications (GSE110711).¹⁴ Beads with containing cDNA were resuspended with whole transcript amplification mixture composed of 2 μL of 10 $\mu\text{mol/L}$ primer mix (trP1 and 3'WTA), 10.5 μL of DW, and 12.5 μL of KAPA Hifi HotStart ReadyMix (KAPA Biosystems). The thermal cycling conditions were programmed as follows: denaturation at 95°C for 3 minutes, 12 cycles of denaturation for 20 seconds

at 98°C, annealing for 15 seconds at 65°C, and extension for 5 minutes at 72°C, followed by a final extension at 72°C for 5 minutes. Next, 25 µL of the first-PCR products were used for purification with an Agencourt AMPure XP kit (Beckman Coulter) at a 0.7:1 ratio of beads to sample and eluted with 15 µL of DW. Fragmentation and adaptor ligation were performed using 10–60 ng of the second-PCR product as a template with NEBNext FS DNA Library Prep Kit (New England Biolabs) with some modifications. NEBNext Adaptor for Illumina in the “adaptor ligation” step was substituted by 1.5 µmol/L CS1 adaptor, and the reaction volume was one fourth of the recommended in all steps. Adaptor-ligated DNA was added with 7.125 µL of 10x TE and then purified using Agencourt AMPure XP kit (Beckman Coulter) at a 0.4:1 ratio of beads to sample to remove large fragments and a 0.7:1 ratio of beads to sample to remove smaller fragments; finally, it was eluted with 20 µL of Tris-HCl (pH 8.0). The second PCR was carried out using barcoded primers to enrich the TCR cDNA flanked with sequencing adapters. The second-PCR mixture consisted of 2.5 µL of 10 µmol/L trP1 primer, 2.5 µL of 10 µmol/L IonA-BC primer, 7.5 µL of template, and 12.5 µL of NEBNext Ultra II Q5 Master Mix (accessory of NEBNext FS DNA Library Prep Kit). The thermal cycling conditions were programmed as follows: denaturation at 98°C for 30 seconds, 11 cycles of denaturation for 10 seconds at 98°C, and annealing and extension for 1 minute 15 seconds at 65°C, followed by a final extension at 65°C for 5 minutes. The PCR product was purified and subjected to size selection using Agencourt AMPure XP kit (Beckman Coulter) at a 0.7:1 ratio of beads to sample and eluted with 20 µL of Tris-HCl (pH 8.0). Amplified TCR libraries were quantified using a KAPA SYBR Fast qPCR Kit (KAPA Biosystems, #KK4621), and size distribution was analyzed by agarose electrophoresis and SYBR Gold staining (Thermo Fisher Scientific, #S11494). Primers used for library preparations are summarized in Table S1.

Final RNAseq libraries, whose lengths were 200–300 base pairs, were pooled and sequenced using an Ion 540 Kit Chef, an Ion 540 Chip kit, and an Ion GeneStudio S5 Sequencer (Thermo Fisher Scientific, # A27759, #A27766, # A38194) according to the manufacturer's instructions, except the input library concentration (65 pmol/L) and flow number (550). The raw data have been deposited at the NCBI GEO; accession GSE154539.

qPCR analysis was performed using a THUNDERBIRD Probe qPCR Mix (Toyobo, #QPS-101) on a QuantStudio 6 real-time PCR system (Applied Biosystems). Sequences of the primers for TRBC are as follows: forward 5'- GCTGTGTTTGAGCCATCAGAA -3', reverse 5'- GTGCACCTCCTTCCCATTCACCC-3', probe 5'- AAGGCCACACTGGTGTGCCTGGCCACAG-3'. TaqMan Gene Expression Assay probes for ACTB (Hs.PT.39a.22214847), GZMB (Hs00188051_m1), IFNG (Hs00989291_m1), PDCD1 (Hs01550088_m1), CD8A (Hs00233520_m1), FOXP3 (Hs01085834_m1), CD274 (Hs00204257_m1), and CD4 (Hs01058407_m1) were purchased from Applied Biosystems. The expression levels of all target mRNAs were normalized against the expression level of ACTB in each sample.

2.9 | Transcriptome data analysis

Adaptor trimming and quality filtering of sequencing data were performed using cutadapt v1.18.¹⁵ Filtered reads were mapped to hg38 Refseq RNA using Bowtie2-3.4.2²⁰ with the following parameters: -t -N 1 -D 200 -R 20 -L 20 -i S,1,0.50 --nofw. Tag numbers of each gene were quantified as the expression level of each gene. Between-sample normalization was performed against raw count data using Microsoft R open 3.6.1 (<https://mran.microsoft.com/open/>) and TCC package (DDD-D method).²¹ Genes with fold change ≥ 4 and maximum expression ≥ 20 were identified as differentially expressed genes. Coexpressed gene modules among differentially expressed genes were detected using the WGCNA package.²² For WGCNA, the power value was 19, the merge threshold value was 0.1, the threshold value for the output of coexpression interactions was 0.25, and other calculation settings were set to defaults. The genes in gene modules associated with partial response (PR) were further clustered into upregulated and downregulated genes in patients with PR using the hclust function of the stats package. Among genes upregulated in PR (1606 genes), genes associated with antitumor immune responses were extracted. If multiple biopsies are obtained at the same time point in a patient, RNAseq and subsequent data processing were performed separately.

2.10 | Statistical analysis

Statistical analyses were performed using GraphPad Prism (ver7) software (GraphPad Software). Unpaired *t*-test was run on the comparison of repertoire parameters between responders and nonresponders. Paired *t*-test was run on the comparison of repertoire parameters between P1 and P3 among responders or nonresponders. *R*-value was calculated as the Pearson correlation coefficient.

3 | RESULTS

3.1 | Number of overlapping clones in the tumor increased in responders following treatment

In this study, the TCR β repertoire of eight patients with advanced gastrointestinal cancer treated with an anti-PD-1 antibody (nivolumab) was analyzed. The best overall responses were the following: two patients with PR, three patients with stable disease (SD), and three patients with progressive disease (PD; Table 1). Hereafter, we defined “responders” as patients whose tumor size decreased (ID1, 2, 5, 13) and “nonresponders” as those whose tumor size increased (ID3, 7, 11, 23). We collected peripheral blood samples enriched with CD4⁺ and CD8⁺ T cells at four time points (P1; day 0, P2; day 21–27, P3; day 39–55, P4; disease progression)

and day-matched biopsies from primary tumor site before (day 0) and after the treatment (day 39-55; Table 1). No viable tumor cells remained in six biopsies collected from four patients determined pathologically (Table 1 and 2). This is presumably due to prior treatments (Table S2).

The TCR repertoire of blood and tumor biopsies was first analyzed separately, and the extent of clonal expansion in each repertoire was quantified in line with previous reports.^{1,6-8,23} We evaluated the clonality of the TCR repertoire, reflecting the extent of the clonal expansion of T cells using the 1-Pielou index.²⁴ There was no association between the blood CD4⁺ and CD8⁺ T-cell repertoire clonality and clinical responses (Figure 1A,B). Regarding tumor biopsies, clonality tended to decrease in both responders and non-responders, while the number of clones in the tumor tended to be higher in responders after treatment (Figure 1C). Clonality and the number of clones in the tumor showed a negative and positive correlation with TCR β mRNA expression level, respectively (Figure 1D). These results suggest that tumor infiltration of a variety of T-cell clones occurs after treatment.

Then, we examined the blood-tumor overlapping T-cell clones in tumor biopsies to analyze the mobilization of T-cell clones from the peripheral circulation. T-cell clones found in the tumor, which also presented in blood CD4⁺ or CD8⁺ repertoire at the corresponding time point, were identified (Figure 2A, left). Then, the number and total frequency of these overlapping clones were calculated (Figure 2B). The number of CD4⁺ and CD8⁺ overlapping clones tended to increase in responders after treatment (Figure 2C). In contrast, the total frequency of CD4⁺ and CD8⁺ overlapping clones did not show clear trends (Figure 2D). The total number of CD4⁺ or CD8⁺ overlapping clones and the change in their number after treatment was correlated with *Cd4* or *Cd8a* mRNA expression levels, respectively. These results suggest that an increase in the number of

overlapping clones reflected an infiltration of T cells into the tumor (Figure 2E,F).

3.2 | TCR repertoire overlap in the blood was greater in responders throughout the treatment

Next, we focused on the blood-tumor overlapping clones in the blood (Figure 2A, right). Responders exhibited a greater number and total frequency of overlapping CD4⁺ or CD8⁺ T-cell clones in the blood before (P1) and after (P2 and P3) treatment (Figure 3A-C). Notably, the correlation between the extent of blood-tumor overlapping clones in the blood and the levels of *Cd4* or *Cd8a* mRNA expression in the tumor was weaker than that between the number of overlapping clones in the tumor and *Cd4* or *Cd8a* mRNA expression levels (Figures 2E and Figure 3D,E). From transcriptome analysis of tumor biopsies (Figure S1), we observed a higher expression of immune-related genes, such as *Cd3e*, *Nfatc1*, and *Tnf*, in patients ID 1 and ID 13 who showed a greater extent of blood-tumor overlap and achieved PR after treatment. Interestingly, patient ID 1 exhibited a higher frequency of CD8⁺ overlapping clones in the blood, while the expression level of immune-related genes in the tumor was equivalent to that of nonresponders before treatment. Therefore, the extent of blood-tumor overlapping clones in the blood did not merely represent the extent of T-cell infiltration in the tumor.

Then, we tried to summarize the pattern of blood-tumor overlap, represented by the number or total frequency of overlapping clones ("OLnumber" or "OLfreq") in blood CD4⁺ or CD8⁺ T cells ("CD4" or "CD8") at three time points ("P1" or "P2" or "P3"). Unsupervised hierarchical clustering using 12 parameters representing the blood-tumor overlap grouped the patients into two clusters (Figure 3F). Three responders (ID 1, ID5, and ID 13) belonged to the

TABLE 1 Characteristics of patients and samples analyzed in this study

Patient characteristics				Peripheral blood (d) ^a				Biopsy sample (d)					
Patient ID	Cancer type	Sex	Age	P1	P2	P3	P4	P1	Presence of tumor tissue	P3	Presence of tumor tissue	Max. change of tumor size ^c	Best response
1	EC	M	71	0	23	44	219	0	- ^b	44	- ^b	-68.8%	PR
2	CRC	F	35	0	21	42	86	0	+	42	+	-8.5%	SD
3	EC	M	57	0	22	55	78	0	+	55	+	50.0%	PD
5	GC	F	64	0	22	42	135	0	- ^b	42	+	-37.5%	SD
7	CRC	M	70	0	23	46	71	0	+		- ^d	22.3%	PD
11	EC	M	80	0	27	39	228	0	+	39	+	6.3%	SD
13	EC	M	80	0	26	49	103	0	- ^b	49	- ^b	-54.5%	PR
23	CRC	F	77	0	21	41	- ^d	0	- ^b	41	+	37.7%	PD

Abbreviations: CRC, colorectal cancer; EC, esophageal cancer; F, female; GC, gastric cancer; M, male; PD, progressive disease; PR, partial response; SD, stable disease.

^aPeripheral blood samples represent both CD4⁺ and CD8⁺ T-cell samples.

^bNo viable tumor cells were found in histopathological tissues analyzed.

^cMaximum change in sum of tumor diameters from baseline, measured by computed tomography.

^dNot sampled.

^eClinical response of patient ID23 was determined by metastatic lesion.

Patient ID	P1	P3
1	Parakeratosis with basal cell atypia ^a	Granulation tissue ^a
2	Adenocarcinoma	Adenocarcinoma
3	Squamous cell carcinoma	Squamous cell carcinoma
5	Parakeratosis and chronic inflammation ^a	Adenocarcinoma
7	Adenocarcinoma	— ^b
11	Squamous cell carcinoma	Squamous cell carcinoma
13	Granulation tissue ^a	Granulation tissue ^a
23	Tubular adenoma ^a	Adenocarcinoma

TABLE 2 Histological features of biopsy samples

^aNo viable tumor cells were found.

^bNot sampled.

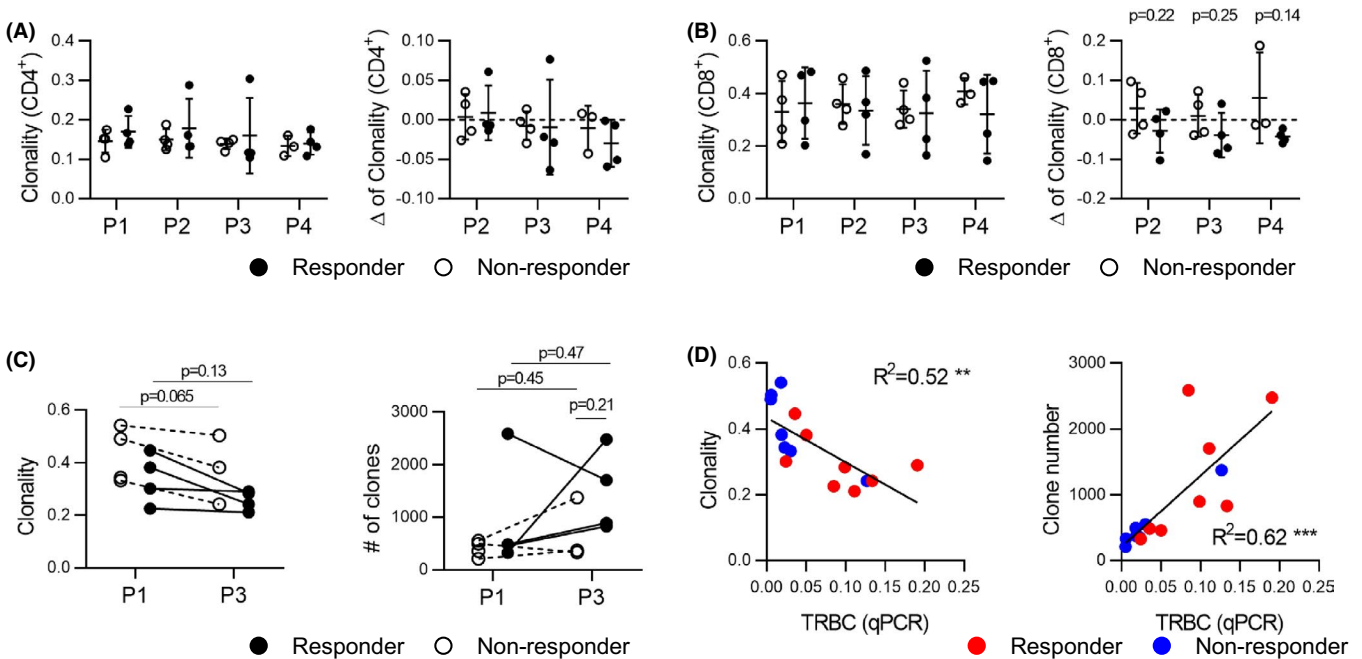


FIGURE 1 T-cell receptor (TCR) repertoire analysis on whole T cells in the blood or the tumor. A and B, Temporal tracking of clonality of blood CD4⁺ (A) and CD8⁺ (B) T-cell repertoire. Raw values (left) and their changes from the baseline (right) are depicted for each patient. Clonality was evaluated by 1-Pielou index. C, Clonality (left) and number (right) of T-cell clones of tumor biopsies. D, Correlation between the mRNA expression level of TRBC and clonality (left) or number (right) of T-cell clones of tumor biopsies. Clonality of the repertoire is calculated as the 1-Pielou index. D, R^2 value, calculated as the square of the Pearson correlation coefficient, is shown on the plot. Clinical response of patients (responders, $n = 4$; nonresponders, $n = 4$) is depicted in the legend. Multiple unpaired *t*-tests (C and D, responder vs nonresponder); paired *t*-tests (C and D, P1 vs P3); ** $P \leq .01$, *** $P \leq .001$

same cluster, in which a higher number of overlapping CD8⁺ T-cell clones in the blood were commonly observed. Principal component analysis of the same 12 parameters was also performed. Principal component 1 (PC1), reflecting the number of overlapping clones in CD4⁺ and the total frequency of overlapping clones in CD8⁺ T cells in the blood, correlated well with the maximum changes in the tumor diameter (Figure 3G and Table 3). Moreover, responders tended to exhibit lower PC1 value than nonresponders (Figure 3H). Overall, these results suggested that blood-tumor repertoire overlap might be a biomarker to classify responders and nonresponders to PD-1 blockade therapy.

3.3 | Emergence of new clones and the expansion of pre-existing clones contribute to the increase in the TCR repertoire overlap

An increase in repertoire overlap in the blood can be explained by (a) the expansion of pre-existing clones and (b) the emergence of new clones. To evaluate these two events separately, we categorized the overlapping clones into “appeared” (not existing in blood at P1, but at P3), “disappeared” (existing in blood at P1, but not at P3), and “persisting” (existing in blood at both P1 and P3) clones, and calculated the number and total frequency in each group. Moreover, persisting

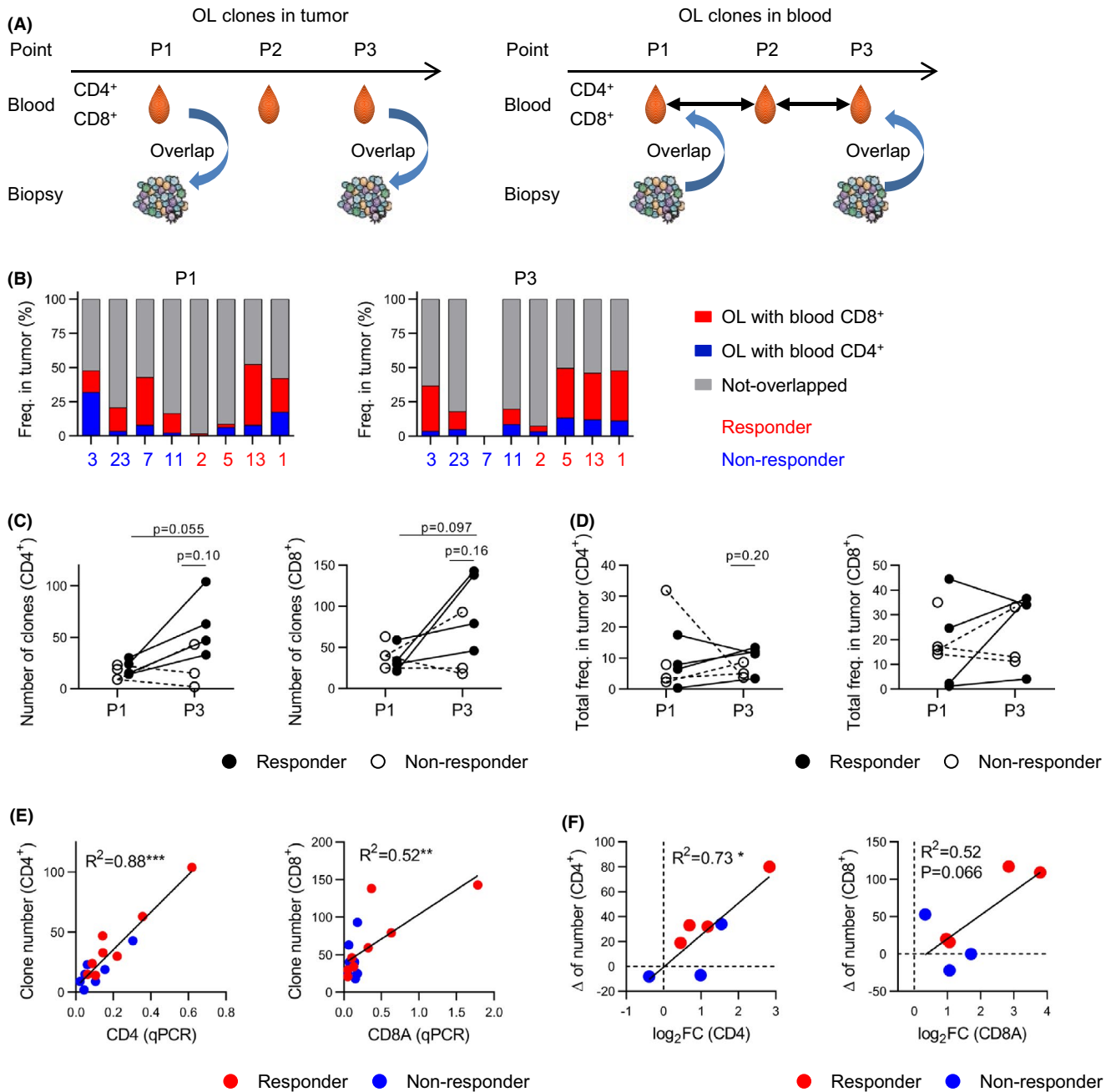


FIGURE 2 T-cell clones in tumor overlapped with the blood. A, Scheme of our analysis on T-cell clones that overlap between the blood and tumor T-cell receptor (TCR) repertoire. First, we identified the T-cell clones in the tumor that also presented in the blood at the corresponding time point (“overlapping clones in the tumor,” left). Next, we identified the T-cell clones in the blood that also presented in the tumor at the corresponding time point (“overlapping clones in blood,” right). B, Frequency of blood overlapping clones in tumor before (P1, left) and after (P3, right) the treatment. Clones that overlapped with blood CD8⁺ (red) or CD4⁺ (blue) T-cell repertoire were colored differently. C, Number of CD4⁺ (left) and CD8⁺ (right) overlapping clones in tumor. D, Total frequency of CD4⁺ (left) and CD8⁺ (right) overlapping clones in the tumor. E, Correlation between the mRNA expression level of CD4 (left) or CD8A (right) and changes in the number of CD4⁺ (left) or CD8⁺ (right) overlapping clones in the tumor. F, Correlation between fold change in the mRNA expression level of CD4 (left) or CD8A (right) and changes in the number of overlapping clones in tumor. E and F, R^2 value, calculated as the square of the Pearson correlation coefficient, is shown on the plot. Clinical response of patients (responders, $n = 4$; nonresponders, $n = 4$) is depicted in the legend. Multiple unpaired *t*-tests (A, B, and C); paired *t*-tests (C, P1 vs P3); * $P \leq .05$, ** $P \leq .01$, *** $P \leq .001$

clones were further grouped into “expanded,” “contracted,” and “unchanged” clones based on the changes in their frequency (Figure 4A, see “Materials and Methods”). Responders exhibited a higher number

of “appeared” CD4⁺ and CD8⁺ T-cell clones (Figure 4B and Figure S2A); however, the proportion of these “appeared” clones in the TCR repertoire overlap was small. “Expanded” clones occupied the largest

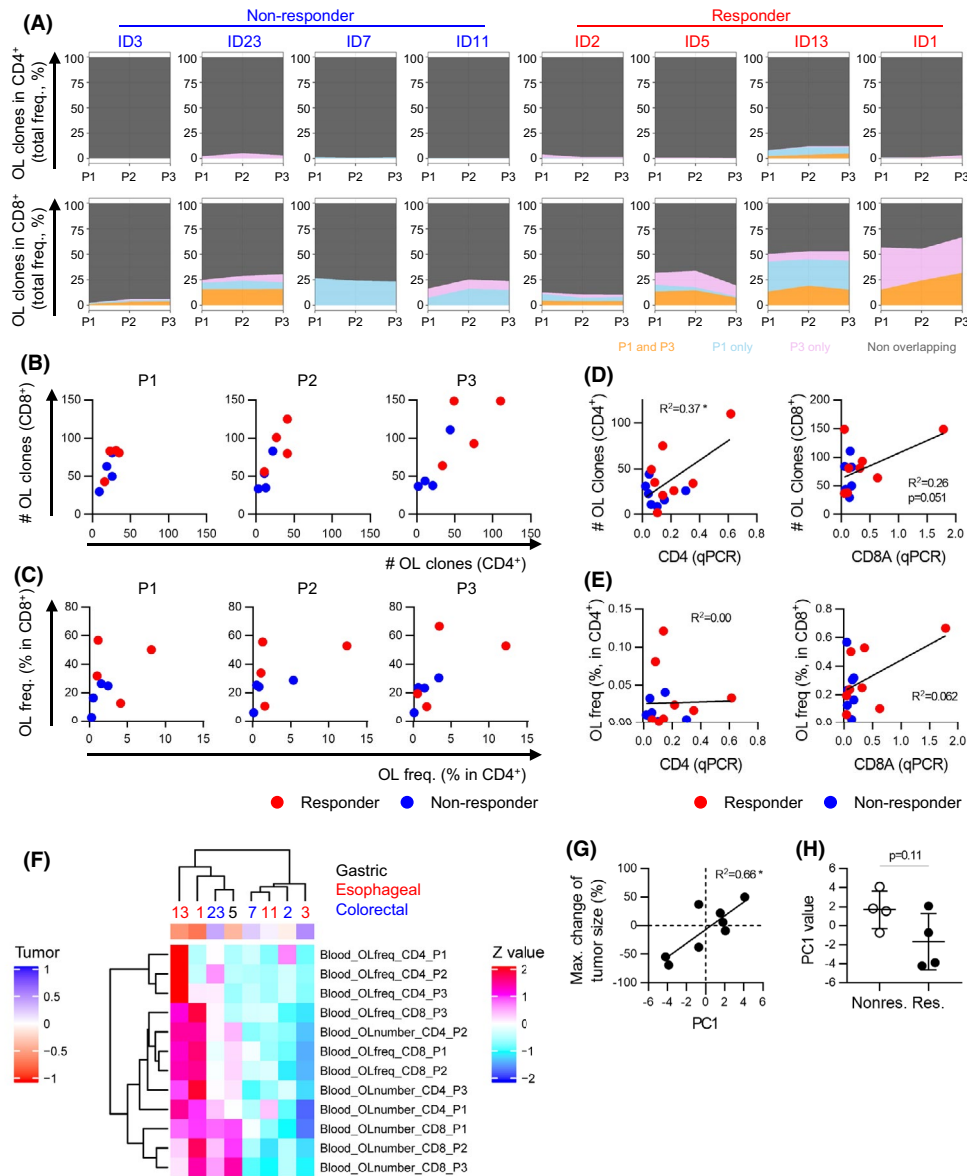


FIGURE 3 T-cell clones in the blood overlapped with the tumor. A, Stackplot for the total frequency of overlapping clones in blood. The total frequency of overlapping clones in blood CD4⁺ (top) or CD8⁺ (bottom) T-cell repertoire was plotted. Overlapping clones were classified based on which time point they presented in the tumor (both P1 and P3, only at P1, or only at P3). The total frequency was calculated for each class and depicted in the legend. B and C, Overlapping clones in blood. Patients are plotted with their number (B) and total frequency (C) of overlapping clones in CD4⁺ (x-axis) and CD8⁺ (y-axis) T-cell repertoire of blood. D, Correlation between the mRNA expression level of CD4 (left) or CD8A (right) in the tumor and the number of CD4⁺ (left) or CD8⁺ (right) overlapping clones in blood. E, Correlation between the mRNA expression level of CD4 (left) or CD8A (right) in the tumor and the total frequency of CD4⁺ (left) or CD8⁺ (right) overlapping clones in blood. F, Heat map of the T-cell receptor (TCR) repertoire parameters following the treatment. Patients are grouped by unsupervised hierarchical clustering based on the Z values of the parameters representing the blood-tumor repertoire overlap. Each row represents a repertoire parameter used in clustering, and each column represents a patient. The maximum changes in the sum of tumor diameter are also plotted as the annotation of each column. Colors of patient IDs indicate the cancer types as in the legend (gastric cancer, $n = 1$; esophageal cancer, $n = 4$; colorectal cancer, $n = 3$). G and H, Principle component analysis on TCR repertoire parameters. Principle components are calculated using parameters of the blood-tumor repertoire overlap. G, Patients are plotted with the value of PC1 and maximum changes in the sum of tumor diameter. H, The value of PC1 was compared between responders (Res.) and nonresponders (Nonres.). Clinical response of patients (responders, $n = 4$; nonresponders, $n = 4$) is depicted as in the legend. Unpaired *t*-tests (H); * $P < .05$

proportion of the repertoire overlap in blood CD8⁺ T cells after treatment in two responders (ID 13 and ID 1; Figure 4C). Notably, ID 13 also exhibited a higher total frequency of expanded clones in blood

CD4⁺ T cells (Figure S2B). These results suggested that both the emergence of new clones and the expansion of pre-existing clones underlaid the increase in TCR repertoire overlap in the blood.

TABLE 3 Correlation between T-cell receptor (TCR) repertoire parameters and the principle components in Figure 3G

Rank ^a	Correlate with PC1	
	Repertoire	R-value ^b
1	Blood_OLnumber_CD4_P2	-0.991
2	Blood_OLfreq_CD8_P2	-0.968
3	Blood_OLfreq_CD8_P1	-0.964
4	Blood_OLnumber_CD4_P3	-0.924
5	Blood_OLfreq_CD8_P3	-0.916
6	Blood_OLnumber_CD4_P1	-0.910

^aThe pairs of principle components and repertoire parameter are ranked according to the absolute value of Pearson's correlation coefficient.

^bPearson's correlation coefficient.

3.4 | Greater extent of blood-tumor repertoire overlap was observed in responders before treatment

Finally, we tested whether the extent of blood-tumor TCR repertoire overlap before treatment is associated with the efficacy of PD-1 blockade. To this end, only the samples collected before the treatment (P1) were used to identify overlapping clones (Figure 5A). First, overlapping CD8⁺ T-cell clones in the blood were identified for all clones present in the tumor. However, no apparent correlation was observed between change in the tumor diameter and the total frequency of overlapping CD8⁺ T-cell clones in the blood (Figure S3A). Then, overlapping clones with frequencies over 0.01% in the tumor were examined to exclude minor clones from the analysis (Figure 5B).²⁵ Considering that small amounts of blood-borne cells exist in the vasculature of tumor tissue,²⁶ filtering minor clones in the tumor TCR repertoire reduced the possible contamination of peripheral blood T cells. We revealed an apparent correlation between tumor diameter changes and the total frequency of overlapping clones in the blood, except for patient ID 7 (Figure 5C). An association between the total frequency of CD4⁺ overlapping clones and the clinical response was not observed (Figure S2B). Collectively, these results suggested that a higher frequency of blood CD8⁺ T-cell clones that a higher frequency of CD8⁺ overlapping clones in blood was indicative of a better clinical response to PD-1 blockade.

4 | DISCUSSION

This study proposed a potential advantage of blood-tumor TCR repertoire overlap analysis for monitoring antitumor T-cell responses following PD-1 blockade. In the tumor, the number of blood-tumor overlapping clones after treatment tended to increase in responders, which was associated with increased T-cell infiltration into the tumor. In the blood, responders exhibited a greater extent of blood-tumor overlapping clones, which was also observed before the treatment when focusing on middle and major clones in the tumor. To our knowledge, this is the first study demonstrating the possible

association of a greater blood-tumor TCR repertoire overlap and favorable clinical responses after PD-1 blockade in gastrointestinal cancer.

An advantage of the blood-tumor overlap analysis is that this analysis can enrich tumor-associated T-cell clones in the blood. The blood TCR repertoire contains clones that are not associated with cancer, such as virus-specific clones²⁷ and autoreactive clones.^{28,29} Thus, it is unclear to what extent the blood TCR repertoire changes represent antitumor T-cell responses during PD-1 blockade therapy. Indeed, the clonality of the blood T-cell repertoire containing both overlapping and nonoverlapping clones exhibited only weak associations with responses to PD-1 blockade in this study. Moreover, recent studies indicate the importance of T-cell clones supplied from outside the tumor for the antitumor effect of PD-1 blockade.^{9,10} Therefore, monitoring the blood-tumor overlap enables evaluation of the replenishment of tumor-reactive T cells from the blood to the tumor. Consistent with these observations and hypotheses, several studies analyzing the TCR repertoire in neoadjuvant ICI treatment have reported that the expansion or emergence of tumor overlapping clones in the blood is associated with better clinical effects.^{30,31} Further studies are needed to examine whether the blood-tumor overlapping T-cell clones actually recognize cancer and contribute to the antitumor effect of PD-1 blockade.

Analyses of the blood-tumor TCR repertoire overlap in the tumor revealed distinct patterns in two patients with PR. One patient, patient ID 1, showed a large amount of overlapping CD8⁺ T-cell clones in the blood and upregulation of gene expression signature related to T-cell activation only after treatment. The other patient, patient ID 13, showed a large amount of overlapping CD4⁺ T-cell clones in the blood and CD8⁺ T-cell clones to a lesser extent. This patient ID 13 exhibited a strong T-cell activation signature in the tumor not only after but even before the treatment, suggesting that pre-existing antitumor responses were presumably mediated by CD4⁺ T cells. Several studies reported a beneficial role of CD4⁺ T-cell responses in the antitumor effect of PD-1 blockade.^{32,33} Importantly, analyzing CD4⁺ and CD8⁺ T-cell repertoires separately made it possible to clarify differences in the dominance of CD4⁺ and CD8⁺ T-cell responses between the two patients with PR. Further studies are required to establish the significance of blood-tumor overlap of CD4⁺ T cells in antitumor responses and the benefit of analyzing the CD4⁺ and CD8⁺ T-cell repertoire separately.

A greater baseline of the blood-tumor overlap in blood CD8⁺ T cells was associated with better clinical responses not only after but also before treatment. One interpretation of this observation is that, in patients with greater blood-tumor overlap, the immune response inside the tumor had previously been activated (ie, "hot tumor"), and the level of T-cell infiltration from the blood into the tumor was high before treatment. However, this was inconsistent with the transcriptome analysis results on biopsies; one patient with PR (ID 1) showed lower expression of genes associated with antitumor T-cell responses, but the proportion of overlapping CD8⁺ T-cell clones in the blood was large before the treatment. Another interpretation is that overlapping clones in

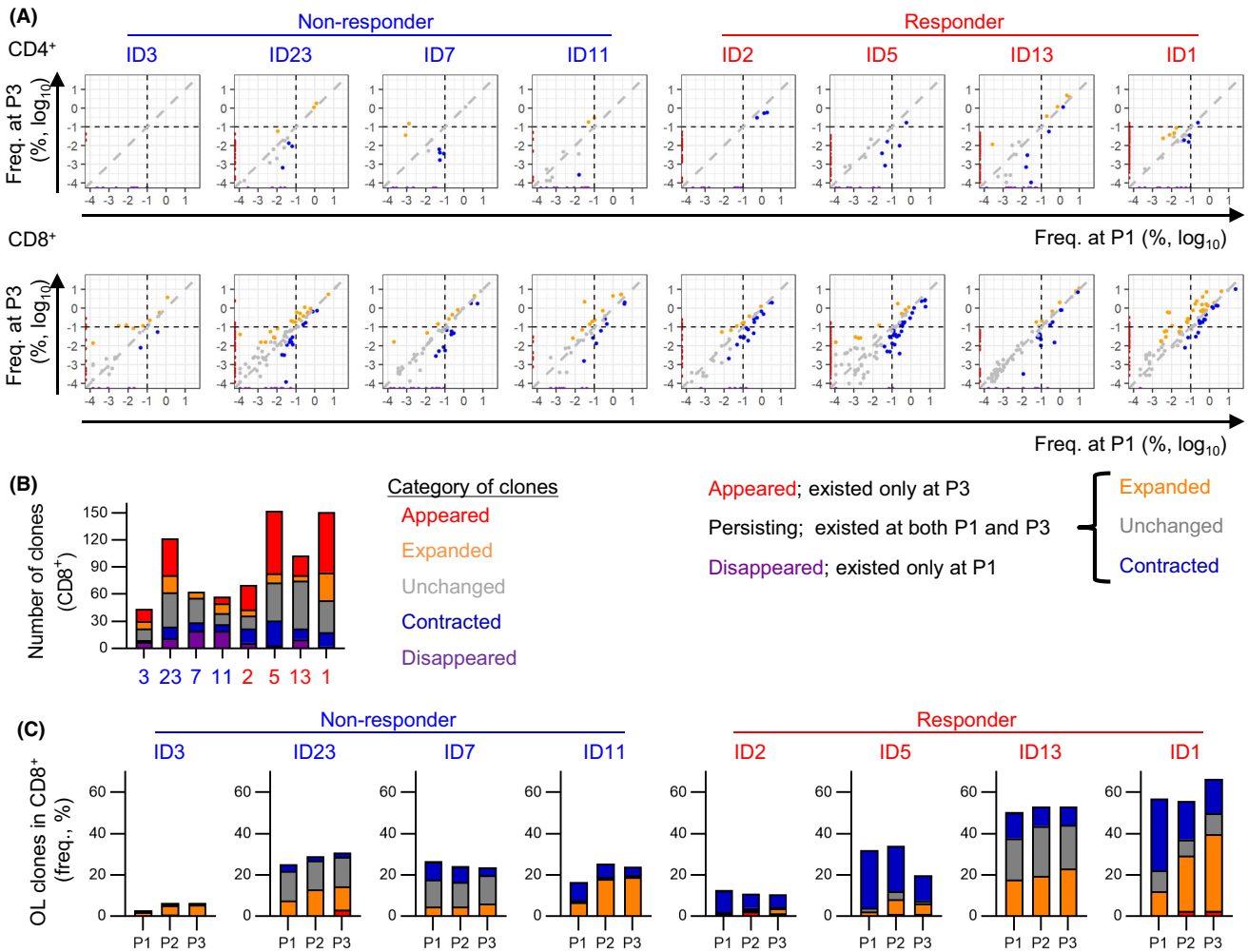


FIGURE 4 Changes in the abundance of individual overlapping clones in blood. A, Scatter plot of overlapping clones in blood CD4⁺ (top) and CD8⁺ (bottom) T-cell repertoire. Each dot on the plot represents a blood-tumor overlapping clone with log₁₀ frequency at P1 (x-axis) and P3 (y-axis). Overlapping clones were categorized into "appeared," "expanded," "unchanged," "contracted," and "disappeared" clones (see "Materials and Methods" section), and depicted by different colors as in the legend. B, Number of overlapping clones in blood CD8⁺ T cells with the changing pattern in their abundance following the treatment. C, Total frequency of overlapping clones in blood CD8⁺ T cells with the changing pattern in their abundance following the treatment. The total frequency of clones in each group is calculated at each time point. Clinical response of patients (responders, n = 4; nonresponders, n = 4) is depicted as in the legend

the blood functioned as a reservoir of tumor-reactive T cells activated by PD-1 blockade. This possibility is supported by previous researches demonstrating that (a) the repertoire of blood CD8⁺ PD-1⁺ T cells show a higher overlap with CD8⁺ PD-1⁺ T cells in the tumor³⁴ and that (b) PD-1 blockade mainly activates CD8⁺ PD-1⁺ T cells in the blood.³⁵ These findings support that the extent of blood-tumor overlapping clones in the blood might represent anti-tumor potential not reflected by immune-related gene expression in the tumor.

One of the main limitations of this study was that some tumor biopsy samples were pathologically determined to lack viable tumor cells, presumably due to prior treatment. However, it has been demonstrated that tumor-reactive T cells remain as tissue-resident memory T cells after removing a tumor, at least in a mouse model.³⁶

Considering this, we hypothesize that the overlapping T-cell clones between the blood and biopsies lacking tumor cells can also be used for monitoring antitumor T-cell responses following PD-1 blockade. Another limitation was the small size of the cohort analyzed. Due to the limited number of patients in this study, it was difficult to get the results with statistical significance by analyzing blood-tumor repertoire overlap. In addition, although we could not find an apparent association between blood-tumor overlap and a specific tumor type (Figures 3F and 5C), it is possible that the extent of blood-tumor overlap was confounded by tumor types. We think similar studies in a larger cohort will answer this question.

Despite these limitations, we suggest the possibility of TCR repertoire analysis and subsequent blood-tumor overlap analysis to predict clinical response to PD-1 blockade. Blood-tumor repertoire

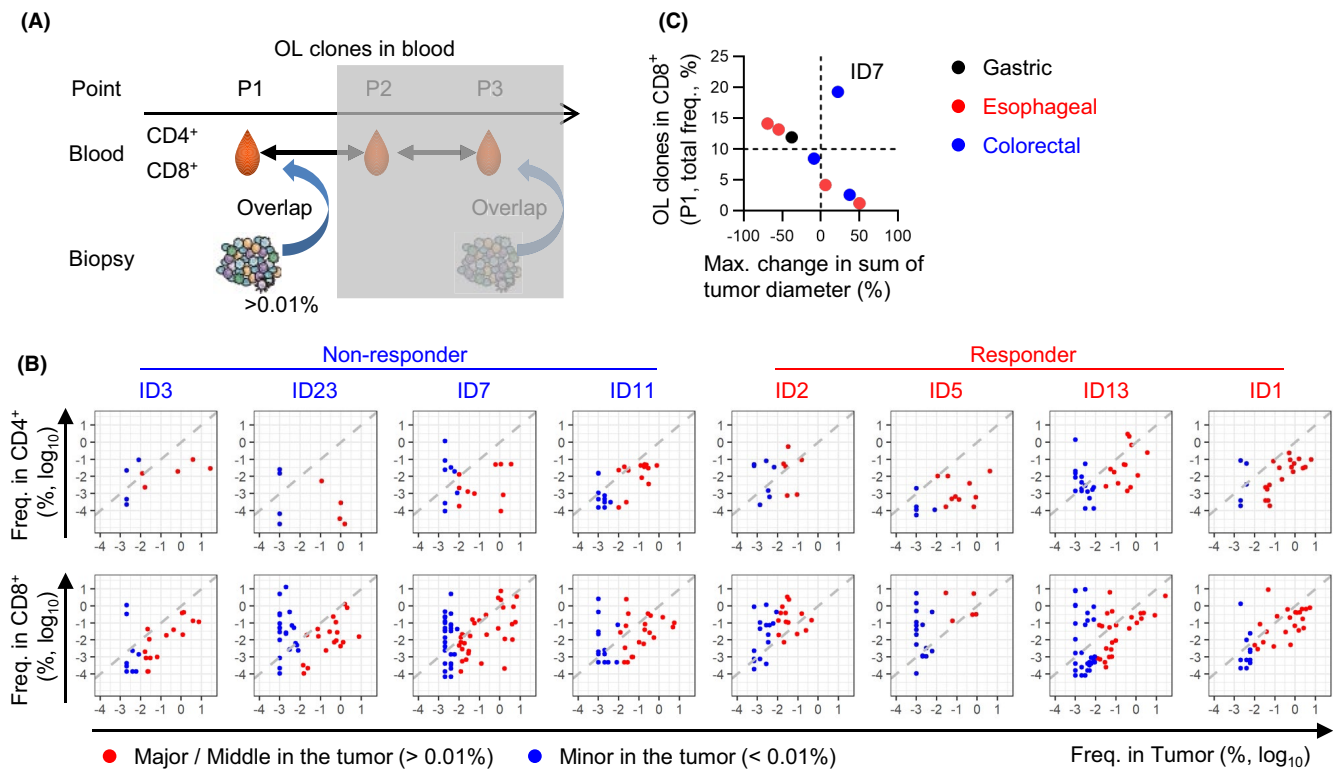


FIGURE 5 Blood-tumor overlapping clones before the anti-PD-1 treatment. A, Scheme of our overlapping repertoire analysis for early prediction of clinical responses. We identified T-cell clones in blood at P1 that also presented in tumor or whose frequency was over 0.01% in tumor at P1. B, Scatter plot of the T-cell clones which overlap between the tumor and the blood. Each dot on the plot represents a single clone with log₁₀ frequency in the tumor (x-axis) and the blood CD4⁺ (upper) or CD8⁺ (lower) T-cell repertoire (y-axis). Colors of overlapping clones represent their abundance in the tumor as in the legend. C, P1 overlapping clones in the blood CD8⁺ T-cell repertoire. Patients were plotted with the maximum changes in the sum of tumor diameter and the total frequency of overlapping clones at P1. The overlapping clones are defined for clones whose frequency is over 0.01% in the tumor. Colors indicate the cancer types of patients as in the legend (gastric cancer, n = 1; esophageal cancer, n = 4; colorectal cancer, n = 3)

overlap seems to reflect tumor-specific T-cell responses of hosts, while PD-L1 expression or TMB represents factors of tumor cells affecting antitumor immune responses. Therefore, blood-tumor repertoire overlap and PD-L1 expression or TMB appear to be complementary, and a combination of these biomarkers can improve the stratification of patients for PD-1 blockade therapy. Further extensive clinical research would establish blood-tumor TCR repertoire overlap as a novel predictive biomarker for PD-1 blockade.

DISCLOSURE

HA reports stock for ImmunoGeneTeqs, Inc. SU reports advisory role for ImmunoGeneTeqs, Inc and stock for ImmunoGeneTeqs, Inc and IDAC Theranostics, Inc. YN reports research funding from Taiho. SS reports advisory role for ImmunoGeneTeqs, Inc and stock for ImmunoGeneTeqs, Inc. AS reports research funding from MSD, Eisai, Ono, Taiho, Takeda, Bayer, Sumitomo Dainippon Pharma, Oncolys Biopharma Inc, and Rakuten Medical Inc. TN reports stock for Killer T save you Inc; consulting or advisory role for OncoTherapy Science, Inc, Takeda, Ono, and Shionogi; speaker's bureau from Janssen, Shionogi, Chugai, Bristol-Myers Squibb Japan, and AstraZeneca; and research funding from BrightPath Biotherapeutics Co. Ltd., Thyas Co.

Ltd., Takeda, Ono, Heartseed Inc, and Noile-Immune Biotech, Inc. TY reports research funding from Novartis Pharma, MSD, Sumitomo Dainippon Pharma, Chugai, Sanofi, Daiichi Sankyo, PAREXEL International Inc, and Ono. KM reports consulting or advisory role for Kyowa-Hakko Kirin, ImmunoGeneTeqs, Inc; research funding from Kyowa-Hakko Kirin, and Ono; and stock for ImmunoGeneTeqs, Inc and IDAC Theranostics, Inc. HN and MS have no conflict of interest to report.

AUTHOR CONTRIBUTIONS

HA, SU, YN, SS, HN, MS, AS, TN, TY, and KM designed the study. YN, HN, AS, and TY performed the clinical study. HA, SU, HN, and MS processed the samples. HA, SU, and SS analyzed data. The initial draft of manuscript was written by HA and SU, with contributions from YN, MS, and KM. All the authors participated in writing the final manuscript.

DATA AVAILABILITY STATEMENT

Availability of data and material; The raw data of TCR repertoire and transcriptome analysis have been deposited at the NCBI GEO; accession GSE154539.

ORCID

Hiroyasu Aoki  <https://orcid.org/0000-0001-7068-715X>

Satoshi Ueha  <https://orcid.org/0000-0002-3871-9921>

Tetsuya Nakatsura  <https://orcid.org/0000-0003-3918-2385>

REFERENCES

1. Tumeq PC, Harview CL, Yearley JH, et al. PD-1 blockade induces responses by inhibiting adaptive immune resistance. *Nature*. 2014;515:568-571.
2. Herbst RS, Baas P, Kim DW, et al. Pembrolizumab versus docetaxel for previously treated, PD-L1-positive, advanced non-small-cell lung cancer (KEYNOTE-010): a randomised controlled trial. *Lancet*. 2016;387:1540-1550.
3. Carbone DP, Reck M, Paz-Ares L, et al. First-line nivolumab in stage IV or recurrent non-small-cell lung cancer. *N Engl J Med*. 2017;376:2415-2426.
4. Havel JJ, Chowell D, Chan TA. The evolving landscape of biomarkers for checkpoint inhibitor immunotherapy. *Nat Rev Cancer*. 2019;19:133-150.
5. Aversa I, Malanga D, Fiume G, Palmieri C. Molecular T-cell repertoire analysis as source of prognostic and predictive biomarkers for checkpoint blockade immunotherapy. *Int J Mol Sci*. 2020;21(7):2378.
6. Yusko E, Vignali M, Wilson RK, et al. Association of tumor microenvironment T-cell repertoire and mutational load with clinical outcome after sequential checkpoint blockade in melanoma. *Cancer Immunol Res*. 2019;7:458-465.
7. Roh W, Chen P, Reuben A, et al. Integrated molecular analysis of tumor biopsies on sequential CTLA-4 and PD-1 blockade reveals markers of response and resistance. *Sci Transl Med*. 2017;9(379):1-24.
8. Fairfax BP, Taylor CA, Watson RA, et al. Peripheral CD8+ T cell characteristics associated with durable responses to immune checkpoint blockade in patients with metastatic melanoma. *Nat Med*. 2020;26:193-199.
9. Yost KE, Satpathy AT, Wells DK, et al. Clonal replacement of tumor-specific T cells following PD-1 blockade. *Nat Med*. 2019;25:1251-1259.
10. Wu TD, Madireddi S, de Almeida PE, et al. Peripheral T cell expansion predicts tumour infiltration and clinical response. *Nature*. 2020;579:274-278.
11. Chen DS, Mellman I. Oncology meets immunology: the cancer-immunity cycle. *Immunity*. 2013;39:1-10.
12. Aoki H, Ueha S, Shichino S, et al. TCR repertoire analysis reveals mobilization of novel CD8+ T cell clones into the cancer-immunity cycle following anti-CD4 antibody administration. *Front Immunol*. 2019;10:1-13.
13. Shitara K, Ueha S, Shichino S, et al. First-in-human phase 1 study of IT1208, a defucosylated humanized anti-CD4 depleting antibody, in patients with advanced solid tumors. *J Immunother Cancer*. 2019;7:1-11.
14. Shichino S, Ueha S, Hashimoto S, et al. Transcriptome network analysis identifies protective role of the LXR/SREBP-1c axis in murine pulmonary fibrosis. *JCI Insight*. 2019;4:e122163.
15. Martin M. Cutadapt removes adapter sequences from high-throughput sequencing reads. *EMBnet. J*. 2013;17:10-12.
16. Schmieder R, Edwards R. Quality control and preprocessing of metagenomic datasets. *Bioinformatics*. 2011;27:863-864.
17. Bolotin DA, Poslavsky S, Mitrophanov I, et al. MiXCR: Software for comprehensive adaptive immunity profiling. *Nat Methods*. 2015;12:380-381.
18. Shugay M, Bagaev DV, Turchaninova MA, et al. VDJtools: unifying post-analysis of T cell receptor repertoires. *PLoS Comput Biol*. 2015;11:1-16.
19. DeWitt WS, Emerson RO, Lindau P, et al. Dynamics of the cytotoxic T cell response to a model of acute viral infection. *J Virol*. 2015;89:4517-4526.
20. Langmead B, Salzberg SL. Fast gapped-read alignment with Bowtie 2. *Nat Methods*. 2012;9:357-359.
21. Tang M, Sun J, Shimizu K, Kadota K. Evaluation of methods for differential expression analysis on multi-group RNA-seq count data. *BMC Bioinformatics*. 2015;16:1-14.
22. Langfelder P, Horvath S. WGCNA: an R package for weighted correlation network analysis. *BMC Bioinformatics*; 2008;9:559.
23. Riaz N, Havel JJ, Makarov V, et al. Tumor and microenvironment evolution during immunotherapy with nivolumab. *Cell*. 2017;171:934-949. e15.
24. Chiffelle J, Genolet R, Perez M, et al. T-cell repertoire analysis and metrics of diversity and clonality. *Curr Opin Biotechnol*. 2020;65:284-295.
25. Wang T, Wang C, Wu J, et al. The different T-cell receptor repertoires in breast cancer tumors, draining lymph nodes, and adjacent tissues. *Cancer Immunol Res*. 2017;5:148-156.
26. Anderson KG, Mayer-barber K, Sung H, Beura L, Britnie R. Intravascular staining for discrimination of vascular and tissue leukocytes. *Nat Protoc*. 2014;9:209-222.
27. Kim J, Kim A-R, Shin E-C. Cytomegalovirus infection and memory T cell inflation. *Immune Netw*. 2015;15:186-190.
28. Vignali D, Cantarelli E, Bordignon C, et al. Detection and characterization of CD8+ autoreactive memory Stem T cells in patients with type 1 diabetes. *Diabetes*. 2018;67:936-945.
29. Ciinciotti BC, Ruggiero E, Campochiaro C, et al. CD4+ memory stem T Cells recognizing citrullinated epitopes are expanded in patients with rheumatoid arthritis and sensitive to tumor necrosis factor blockade. *Arthritis Rheumatol*. 2020;72:565-575.
30. Zhang J, Ji Z, Caushi JX, et al. Compartmental analysis of T-Cell clonal dynamics as a function of pathologic response to neoadjuvant PD-1 blockade in resectable non-small cell lung cancer. *Clin Cancer Res*. 2020;26:1327-1337.
31. Blank CU, Rozeman EA, Fanchi LF, et al. Neoadjuvant versus adjuvant ipilimumab plus nivolumab in macroscopic stage III melanoma. *Nat Med*. 2018;24:1655-1661.
32. Zuazo M, Arasanz H, Fernández-Hinojal G, et al. Functional systemic CD 4 immunity is required for clinical responses to PD -L1/ PD -1 blockade therapy. *EMBO Mol Med*. 2019;11:1-14.
33. Oh DY, Kwek SS, Raju SS, et al. Intratumoral CD4+ T cells mediate anti-tumor cytotoxicity in human bladder cancer. *Cell*. 2020;181:1612-1625. e13.
34. Gros A, Parkhurst MR, Tran E, et al. Prospective identification of neoantigen-specific lymphocytes in the peripheral blood of melanoma patients. *Nat Med*. 2016;22:433-438.
35. Huang AC, Orlowski RJ, Xu X, et al. A single dose of neoadjuvant PD-1 blockade predicts clinical outcomes in resectable melanoma. *Nat Med*. 2019;25:454-461.
36. Malik BT, Byrne KT, Vella JL, et al. Resident memory T cells in the skin mediate durable immunity to melanoma. *Sci Immunol*. 2017;2:eaam6346.

SUPPORTING INFORMATION

Additional supporting information may be found online in the Supporting Information section.

How to cite this article: Aoki H, Ueha S, Nakamura Y, et al.

Greater extent of blood-tumor TCR repertoire overlap is associated with favorable clinical responses to PD-1 blockade.

Cancer Sci. 2021;112:2993-3004. <https://doi.org/10.1111/cas.14975>